A. Zanoni, P. Garbo, G. Quaranta
Online Evaluation of Helicopter Pilot Workload During Flight Simulator Experiments
in: AIAA Scitech 2022 Forum, AIAA, 2022, ISBN: 9781624106316, p. 1-16, AIAA 2022-0511
[AIAA Scitech 2022 Forum, San Diego, CA, USA & Virtual Conference, 3-7 Jan. 2022]
doi:10.2514/6.2022-0511

Online evaluation of helicopter pilot workload during a flight simulator experiment

A. Zanoni*, P. Garbo† and G. Quaranta‡
Politecnico di Milano, Milano, 20156

Enabling the assessment of pilot workload during flight could have very important consequences in enhancing flight safety, especially in rotorcraft, providing the tools for preventive actions against loss of situational awareness and, indicating the possible insurgence of adverse coupling interactions between the pilot and the vehicle. To assess and develop reliable indicators of pilot workload, to be used during flight, first the results of a SHOL operations flight simulation test campaign are analyzed, focusing on the pilot control activity in the time and frequency domain. Subsequently, to enlarge the available dataset, the development of a purposely-designed grip pressure measurement device is presented, along with the preliminary results obtained in a test campaign conducted at the Politecnico di Milano FRAME-Lab helicopter flight simulation facilities, aimed at evaluating the correlation between grip pressure and workload.

I. Nomenclature

RPC	=	Rotorcraft-Pilot Coupling
PIO	=	Pilot-Induced Oscillation
PAO	=	Pilot-Assisted Oscillation
FTIR	=	Frustrated Total Internal Reflection
SHOL	=	Ship Helicopter Operational Limitations
MTE	=	Mission Task Element
MTOW	=	Maximum Take-Off Weight
TOW	=	Take-Off Weight
IAS	=	Indicated Airspeed
GS	=	Ground Speed
ASL	=	Above-Sea Level
LDP	=	Landing Decision Point
FCS	=	Flight control system
PFD	=	Primary Flight Display
CWT	=	Continuous Wavelet Transform
DWT	=	Discrete Wavelet Transform

II. Introduction

Interest in aircraft pilots' workload assessing methods and devices has held a central role in the research on human-aircraft interaction for several decades[1]. In many accidents and incidents occurring during flight, workload plays a very important role, especially as a triggering factor for the subsequent loss of situational awareness, the insurgence of interaction phenomena like Pilot Induced Oscillations (PIOs) or Pilot Assisted Oscillations (PAOs)[2].
In rotorcraft, the latter goes under the general umbrella of Rotorcraft-Pilot Couplings (RPCs). PAOs are especially significant for rotary-wing aircraft, since they are generally subjected to a higher level of vibration. The latter, acting as a source of excitation, can be mediated through the biodynamical response of the pilots' bodies to produce further, often unwanted, control inputs, that can be detrimental in adverse cases [3, 4].

*Post doctoral fellow, Department of Aerospace Science and Technology, via La Masa 34, 20156 Milano.
†PhD student, Department of Aerospace Science and Technology, Via La Masa 34, 20156 Milano.
‡Full Professor, Department of Aerospace Science and Technology, via La Masa 34, 20156 Milano.

The relationship between the task difficulty – and thus the pilot workload – and the insurgence of adverse rotorcraft-pilot couplings has been the subject of significant research work in the past several years [5–7]. It is well-understood that a correlation exists, with task difficulty and instantaneous workload driving a change of pilot control strategies and the related neuromuscular activity.

On the other hand, balancing the workload of the pilot is considered to be an important factor contributing to the pilot's performance during flight operations [8]. Loss of situational awareness can arise from the extreme conditions of workload levels being *too low* or *too high*.

Assessing the pilot instantaneous workload will allow for a greater understanding of the relationship between workload and pilot performance, loss of situational awareness avoidance and prevention, detection and managing of adverse interactions between the pilot behavior (both active and passive, the latter represented by the body biodynamics) and the aircraft dynamics. Additionally, the possibility to measure objectively instantaneous workload levels while performing a task will allow us to compare, at every instant in time, a simulated flight with a real flight also in terms of pilot workload and not only in terms of similarities of the aircraft response. This could be particularly important when simulation is used for certification [9].

Workload assessment, currently, is primarily done via subjective assessment that the pilot performs as close as possible to the conclusion of a mission. The assessment is very often supported by purposely-developed charts, e.g. the Bedford rating scale [1] or the more specialized DIPES scale [10]. In the first case, the assessment is based on the pilot's spare ability to perform tasks non-directly related to piloting, while in the second case on the evaluation of the compensation effort required to perform the task. In virtually all the subjective methods, the pilot assessment should be related to a single Mission Task Element (MTE), for it to be related to a mission segment that will present a uniform level of requirements to the piloting task.

Two strategies are generally employed, instead, for instantaneous pilot workload assessment:

1) analysis, generally performed in the time domain, of pilot activity, on available data streams like control inputs (as an example, the phase aggression criterion can be cited [6]);
2) the analysis of physiological indicators, via the introduction of specialized measurement devices (e.g. heart rate monitoring, surface electrical capacitance, etc. . .)

In this work, attention was focused on workload assessment through both methods: the first was applied to the analysis of data collected during simulator tests aimed at Ship-Helicopter Operating Limitations (SHOL) assessment, while the second was pursued by developing an innovative hand-grip pressure sensor, to be integrated in the FRAME-Lab helicopter flight simulation facilities at Politecnico di Milano Department of Aerospace Science and Technology.

A. Outline of research

Data collected during a SHOL test campaign, conducted at the Leonardo Helicopter AWARE simulation facility, have been analyzed to search for correlations among the subjective workload ratings, represented by Bedford and DIPES scale ratings, and indicators based on time and frequency analysis of the collected control input signals. Analysis of the same experimental dataset, presented in [7], as noted above, has prompted further research on the relationship between instantaneous task workload and variations in the Neuromuscular Admittance (NMA) and Biodynamc Feedthrough (BDFT) of the pilot-aircraft coupled system.

To further enhance the comprehension of these aspects, the authors have also developed a novel measurement device, based on the optical effect of Frustrated Total Internal Reflection (FTIR), able to produce a signal proportional to the pressure applied by the pilot hands on the control inceptor grip. A patent application regarding the measurement device concept has been filed [11].

The device has been installed on the control inceptors of the FRAME-Lab simulation facilities of Politecnico di Milano Department of Aerospace Science and Technology (DAER). A first experimental campaign devoted to the assessment of the grip pressure as an indicator of the instantaneous pilot workload has been performed, as described in Section V. Preliminary results indicate that the device can provide important information regarding the hand activity of the pilot, and hints at possible paths to identify the pilot instantaneous workload was found in the collected data, as detailed in Section VI.

III. Analysis of SHOL simulations

An experimental campaign involving simulated deck landings of medium-sized five-bladed main rotor helicopters on a Sirio class frigate was conducted on the Leonardo Helicopters AWARE fixed-base simulator test facility in Cascina Costa (Milano, Italy). Tests were performed by a professional test pilot with extensive experience in SHOL operations[7].

Two different helicopters, with TOW of 6000 kg and 7500 kg respectively, were employed. The mission profile has been generated to simulate an approach and deck landing to the ship, at anchor or in forward motion at 12 kn, with a straight stern approach from 400 ft, 50 kn IAS initial trimmed conditions. The mission is composed of the following Mission Task Elements (MTEs):

1) initial descent and decrease of forward flight speed, from the initial trimmed conditions at 400 ft ASL, 50 kn IAS to a Landing Decision Point (LDP) located at 50 ft ASL and GS matching the one of the ship, with a lower limit of 10-15 kn;
2) from the LDP, approach to the ship unit either with a straight-in approach from the stern, or move alongside the landing deck ("hover alongside" approach);
3) wait in hovering conditions for the motion of the ship to dampen and reach a *quiescence* period;
4) perform the final touchdown maneuver.

The mission difficulty, and thus the pilot workload, was modulated varying several parameters regarding the mission, the ship, and the helicopter:

- the ship attitude motion, both in roll and pitch, induced by sea state, varied between 0(calm) and 5 (rough), Douglas scale [12];
- the ship forward motion, varied among null (at anchor) to 12 kn;
- the aircraft TOW, varied between nominal and MTOW configurations;
- the aircraft CG location, varied between nominal and full-aft configurations;

The pilot was asked, immediately after each trial, to score the workload rating for the entire mission, under the presumption that the most relevant MTEs for this aspect were number 3) and 4). This hypothesis was confirmed by the pilot. Scores were given using both the Bedford [1] and the DIPES (standing for Deck Interface Pilot Effort Scale)[10, 13] rating scales.The first is a generic, very well-established rating scale based on the evaluation of the spare ability of the pilot to perform secondary tasks during flight, indirectly evaluating the workload required by the piloting task. The DIPES scale is based on the Cooper-Harper scale [1] but is specific to helicopter-ship operations and focuses on evaluating the guidance compensation effort needed from the test pilot.
A more complete description of the performed tests and the related analysis can be found in [7, 14, 15].

A. Workload analysis

Time histories of the control input on the collective, lateral cyclic and longitudinal cyclic channels were analyzed to extrapolate synthetic indicators correlated to the pilot workload. In the present work, indicators obtained calculating quantities related to descriptive statistical parameters on sliding windows have been considered. The possible usage of time-frequency analyses based on the Wavelet transform is only briefly touched upon in section subsection III.C. At the present state, this latter option constitutes one of the primary research focus the authors would like to pursue in the future developments of the project.

As an example, in Fig. 1, time histories collected during a medium workload (Bedford score 4, DIPES score 3 (VHFD)) trial of the collective control input – represented by the control loading actuator travel – of the helicopter trajectory in the horizontal plane and its altitude are shown. In the trial, the ship was at anchor, with sea state 5 and 25 kn, aligned with the ship heading. It can be seen that the portion of the test after the LDP, i.e. in the approach and deck landing phases, is showing an increased pilot activity on the collective control.

Two possible paths to the definition of indicators of pilot workload, respectively in the time and in the time and frequency domain, are represented in Fig. 2 and Fig. 3. In the former, the aggression $A(\delta)$, is compared to an indicator based on a moving median applied to the signal absolute variation of its moving average. The aggression is defined as [6]

$$A(\delta) = \frac{1}{T}\int_{t}^{t+T} |\dot{\delta}| dt \tag{1}$$

where $\dot{\delta}$ is, in this case, represented by the time derivative (evaluated numerically) of simulator collective control loading actuator travel $\dot{\theta}_0$. The aggression was calculated at each time step using a moving window size of 1 s.
The indicator $M_m(|\delta - \overline{\delta}|)$ is obtained by calculating the moving median applied to the signal obtained by subtracting from the collective signal its moving average $\overline{\delta}$. The median is calculated on a moving window of 1 s and the same window is used for the moving average. In Fig. 2, the indicator is shown in blue in the central graph, and it is compared to its moving average, calculated on moving windows of 2 s width, depicted in red and indicated by the symbol $\overline{M}_m(\delta - \overline{\delta})$. It can be seen that, in this case, the information conveyed by the aggression and the proposed indicator is similar, with the moving average of the latter providing (as expected) a smoother evolution in time.

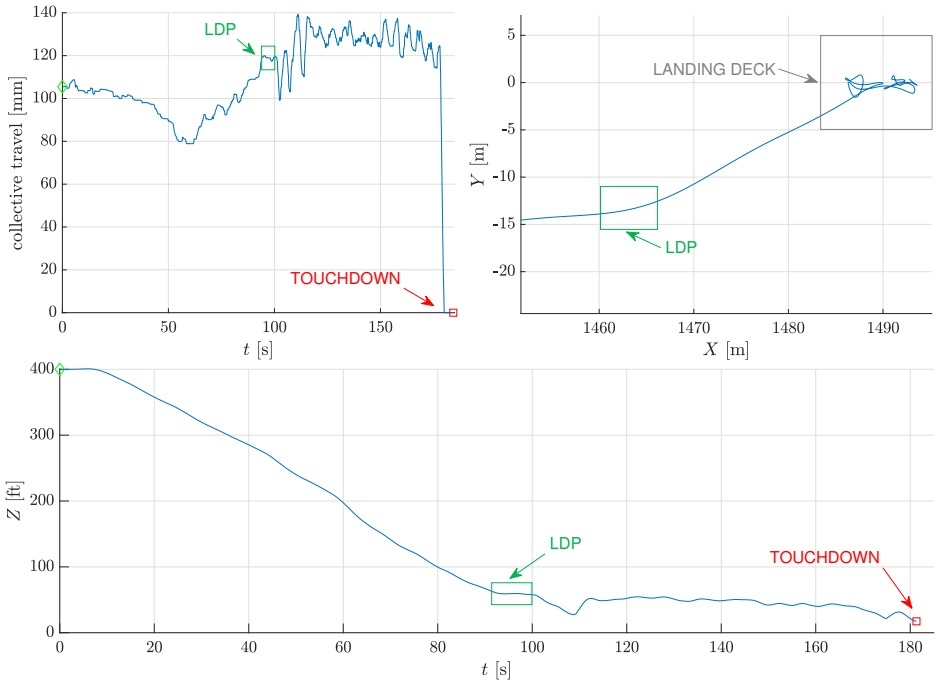

Fig. 1 Excerpt of the collected data during a simulated deck landing: collective input (top-left) compared to the projection in the horizontal plane of the aircraft trajectory (top-right) and to the aircraft altitude AGL (bottom).

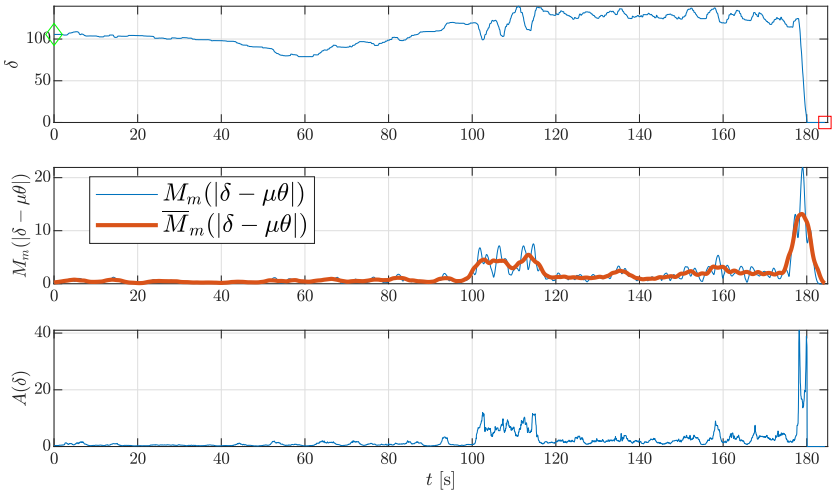

Fig. 2 Comparison between aggression (bottom) and the $I_{\sigma_m}(\theta_0 - \overline{\theta}_0)$ indicator, based on the moving standard deviation calculated on a 1 s window (blue line, middle). The red line represents the moving average of the indicator, calculated on a 2 s sliding window.

Indicator	Symbol	Definition
Aggression	$A(\delta)$	$\frac{1}{T}\int_t^{t+T} \lvert\dot{\delta}\rvert dt$
Moving median absolute deviation	$M_{AD}(\delta)$	$M_e(\lvert\delta_i - M_e(\delta)\rvert)$
Moving variance	$M_{\sigma^2}(\delta)$	$\frac{1}{N-1}\sum_{i=1}^{N}(\delta_i - \mu_N(\delta))^2$
Moving standard deviation	$M_{\sigma}(\delta)$	$\sqrt{\frac{1}{N-1}\sum_{i=1}^{N}(\delta_i - \mu_N(\delta_i))^2}$
Moving median of signal absolute variation	$M_m(\lvert\delta - \mu(\delta)\rvert)$	$M_e(\lvert\delta_i - \mu_N(\delta)\rvert)$

Table 1 Descriptive statistical indicators used in the workload analysis of SHOL simulator tests control inputs. The symbol $Me(\delta)$ indicates the median of signal $\delta(t)$ and $\mu_N(\delta)$ indicates the moving average, calculated on N samples, of signal $\delta(t)$

B. Time-based analysis

Table 1 summarizes the 6 indicators that were applied to the control input time histories to evaluate the pilot activity characteristics and therefore their "instantaneous" workload ratings. Notice that in the table $Me(\delta)$ indicates the median of signal $\delta(t)$ and $\mu_N(\delta)$ indicates the moving average, calculated on N samples, of signal $\delta(t)$. Each indicator was calculated on sliding windows of size equal to 1 s. For each simulator run in the complete dataset featuring a "straight-in" approach, all 6 indicators have been computed on the time histories of the control inputs. The resulting indicator waveforms were numerically integrated into the portion of the signals after the LDP (Cf. Fig. 1). The LDP point was a-posteriori identified as the instant corresponding to the first drop of the aicraft AGL altitude below 50 ft. The synthetic figure of merit obtained by the integration was rescaled in the [0 10] range and compared to the Bedford rating assigned to the individual run – meaning on the most relevant MTEs of the run itself. The results, in terms of Pearson correlation coefficients, is shown in Fig. 4 and Fig. 5. The former, Fig. 4, contains the results obtained by calculating the workload indicators directly to the control input signals, while the latter, Fig. 5, contains the results obtained calculating the workload indicators on the signal derivatives. To do so, the input signals were numerically estimated through a simple forward-differences method. Notice that the aggression $A(\delta)$ is by definition intended to be applied to the control input velocity, therefore the indicator applied to the control input derivative, $A(\dot{\delta})$) is applied on the second derivative of the original signal, in this case.

Of the indicators applied directly on the control input, the ones showing the best performance in terms of correlation with the Bedford rating are the aggression $A(\delta)$, and the moving median applied on the moving absolute deviation $M_m(|\delta - \mu(\delta)|)$.

It can however be noted that the best results are, as one might expect, generally obtained by indicators involving the control input derivative, as is clear by the overall better correlation figures shown by the indicators in Fig. 5. This behavior confirms the good performance shown by the aggression indicator $A(\delta)$ in the previous case.

It can be also noted that while in general the spread of the indicator levels about their average, for a given Bedford rating, is relatively large, some indicators perform better than others in this aspect. For example, $M_{\mathrm{AD}}(\delta)$ and $M_{\mathrm{AD}}(\dot{\delta})$ seem to show a moderately reduced spread compared to other indicators. A detailed analysis of the variance of the indicators will be the subject of further investigations.

C. Time-frequency analysis

A further approach, based on evaluating the frequency content of the signal in a time-depending manner, is exemplified in Fig. 3. The magnitude scalogram of the Continuous Wavelet Transform (CWT) of the collective signal is shown: in the part of the time history related to the most challenging MTEs - namely, hovering waiting for ship quiescence, and deck landing - the frequency content in the higher frequency band increases. It is possible, therefore, to define indicators related to the integral of the magnitude scalogram in the frequency bands of interest, to obtain a measure of the *current* activity of the pilot on the control inceptors, in turn proportional to the *current* workload. This approach will be pursued in the future developments of the research project.

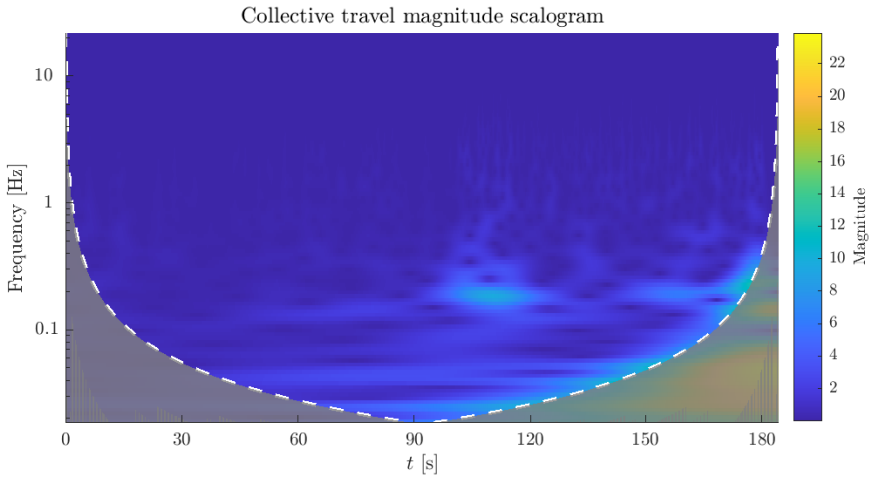

Fig. 3 Magnitude scalogram of the continuous wavelet transform of the collective travel signal. It can be seen that in the latter portion of the signal, corresponding to the higher workload MTEs, is the one showing a greater harmonic content in the higher frequency bands.

IV. Grip pressure sensors

To enhance the available dataset related to both pilot workload and the (correlated) change of *instantaneous* neuromuscular admittance of the pilot body at the control inceptors, a dedicated pressure sensor has been developed and seamlessly integrated into the helicopter grips. The driving concept behind the measuring device development is enabling the evaluation of the overall pressure exerted by the pilot hands on the control inceptors grips, under the hypothesis that it constitutes a representative signal of the pilot workload.

The sensor layout hereafter presented, for which a patent application has been filed [11], relies on an optical working principle commonly referred to as "Frustrated Total Internal Reflection" (FTIR). It consists of a light source located at the center of the grip and probes that are in contact with it and that sense the exerted forces. As shown in Fig. 6(a), the sensor is mainly composed by the indicated four parts: a transparent cylinder (1), illuminated on the two bases by LEDs as to result in total internal reflection inside it (2): this assembly represents the central light source. The probes are formed by an elastic transparent hemispherical shell (3) and a photoresistor (4) installed beneath it. Slots are created in the grip so that the probes can be inserted: they are covered and held in place by a part that completely resembles the shape and material of the rest of the grip so that the final result does not present any major difference in ergonomics from the original device. The CAD of the 3D printed prototype is shown in Fig. 6(b). It is a cyclic grip, with four pressure sensors placed to measure the hand activity of the pilot during the simulated flight in both the lateral and longitudinal direction.

The output signal voltage ranges from 0 to 5 V. It is proportional to the light intensity passing through the probe, which in turn is proportional to the area of contact between the central light source and the spherical shell. The latter varies according to the exerted pressure by the pilot hand.

The relation between the exerted force and the obtained voltage signal is close to linear, as proven by the calibration test, which result is shown in Fig. 7.

The first tests confirmed that the sensor can be a useful tool to quantify the workload evolution in time during a simulated flight experiment: the latter consisted of a small-size helicopter flight which included a cruise part followed by low-altitude precision hovering task. Data from the sensorized grip shows an increased force exerted and a much greater pressure variance in the most demanding part of the flight as shown in Fig. 8, proving thus that such set of sensors can provide an additional data set to investigate the workload evolution during flight [16].

V. Test campaign

The experimental campaign is performed exploiting the motion platform available at the FRAME-Lab laboratories of Politecnico di Milano: it is a six-degrees of freedom base actuated by electric motors. In the present case, the motion is predetermined and acts as a disturbance for the pilot during the MTEs execution. The grips are installed on the motion platform control sticks and are located in front of monitors, in which a simple Primary Flight Display (PFD) is displayed.

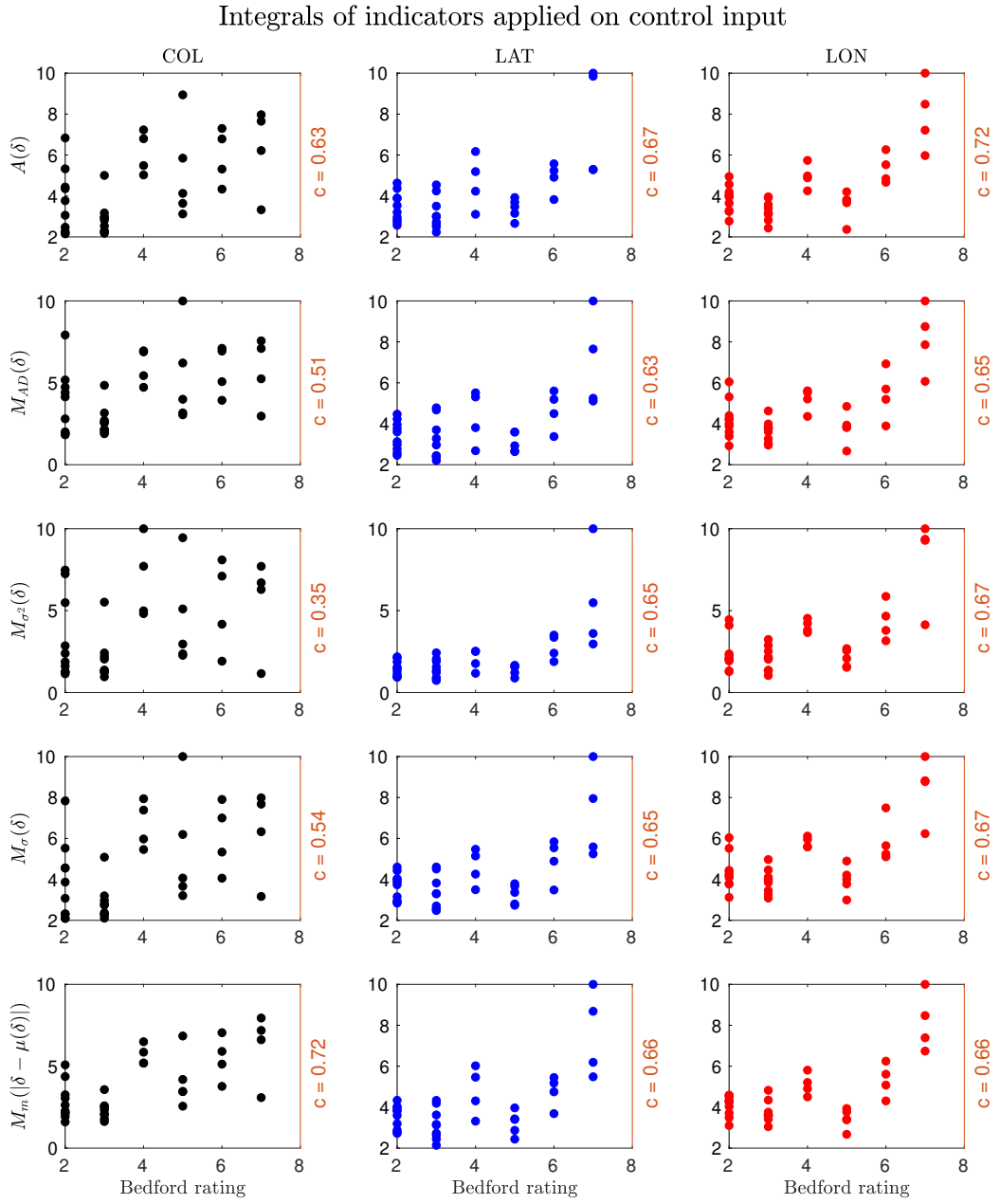

Fig. 4 Workload indicators (Cf.Table 1) calculated on the control input signals of the collective (COL), lateral cyclic (LAT), and longitudinal cyclic (LON) channels. Each plot shows the integral of the indicator in the latter portion of the simulator run, corresponding to the final phases of approach, hovering, and deck landing, to which the Bedford workload rating, shown on the abscissa, is related. The Pearson correlation coefficient c between the indicator integral and the Bedford rating is shown on the right side of each graph.

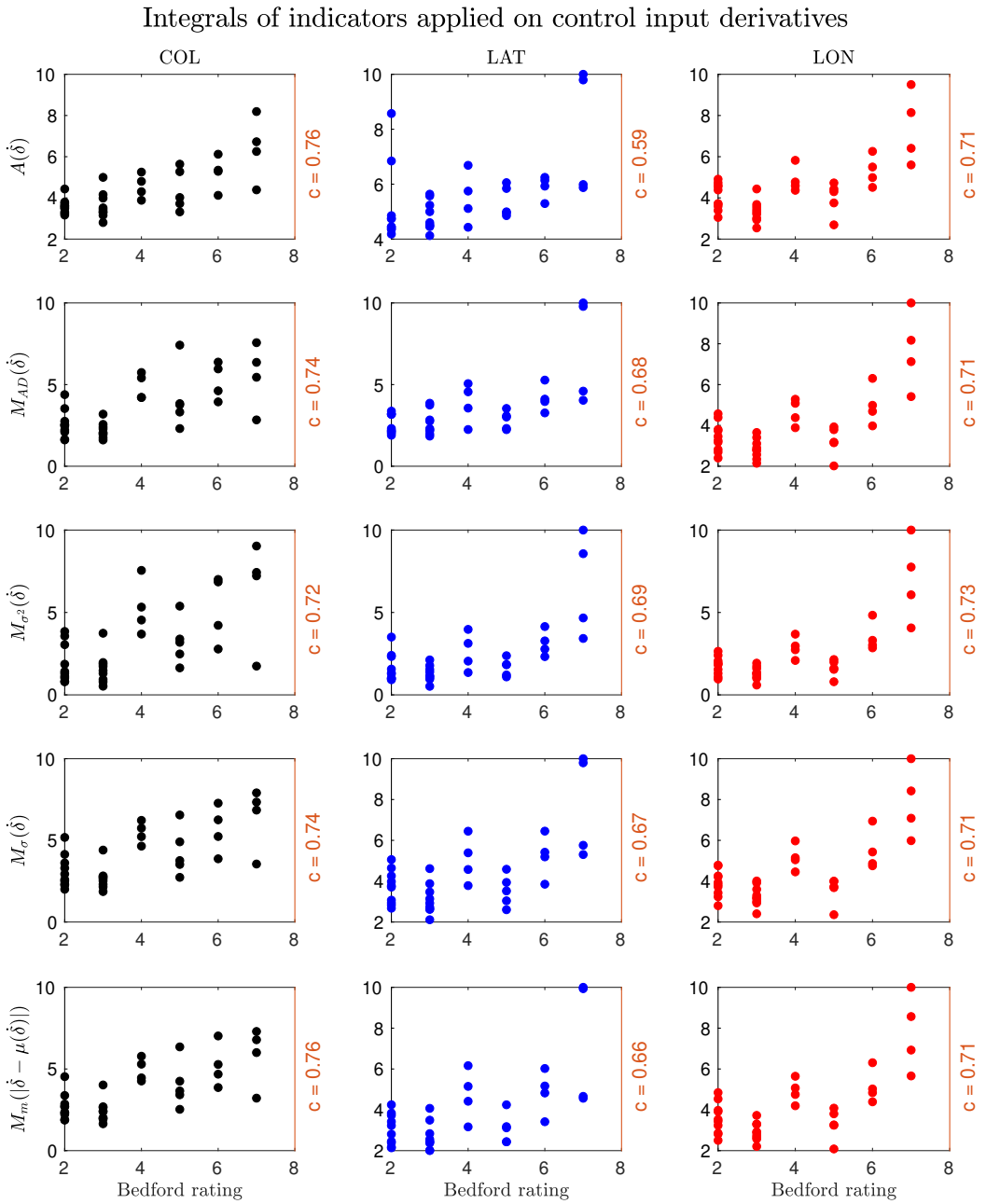

Fig. 5 Workload indicators (Cf.Table 1) calculated on the control input signals numerical derivatives. As in the previous figure, each plot shows the integral of the indicator in the portion of the run after the LDP. Bedford ratings are again shown on the abscissa, and as in Fig. 4 the Pearson correlation coefficient c between the indicator integral and the Bedford rating is shown on the right side of each graph.

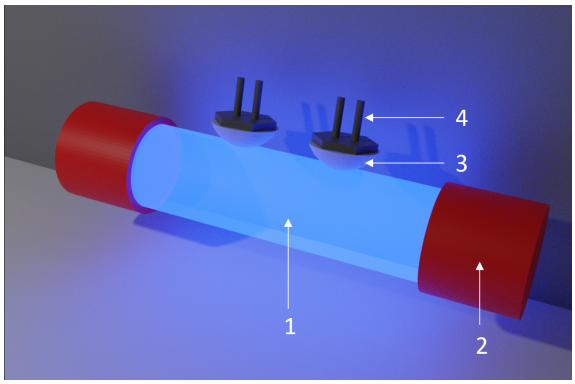

(a)

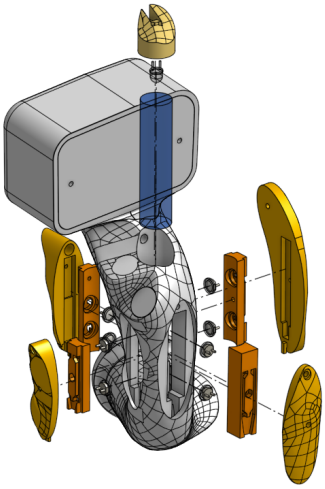

(b)

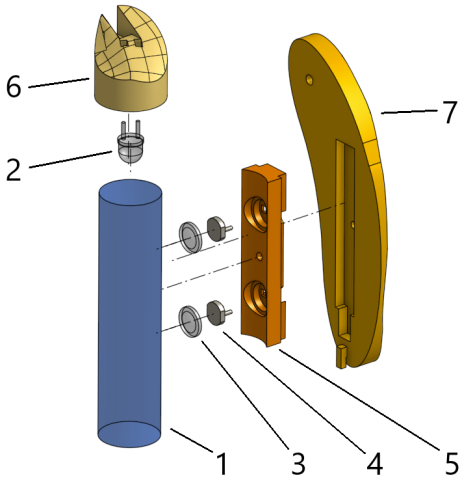

(c)

Fig. 6 Sensor main parts (a) and 3D printed grip prototype (b), with four pressure sensors. In (c) the elements of the OPT-IN sensor are shown in detail: the central transparent medium (1), the LED illuminating it as to form total internal reflection (2), the hemispherical probes (3), the photoresistor (4), the case of the probes (5), the LED cap (6) and sensor outer shell (7).

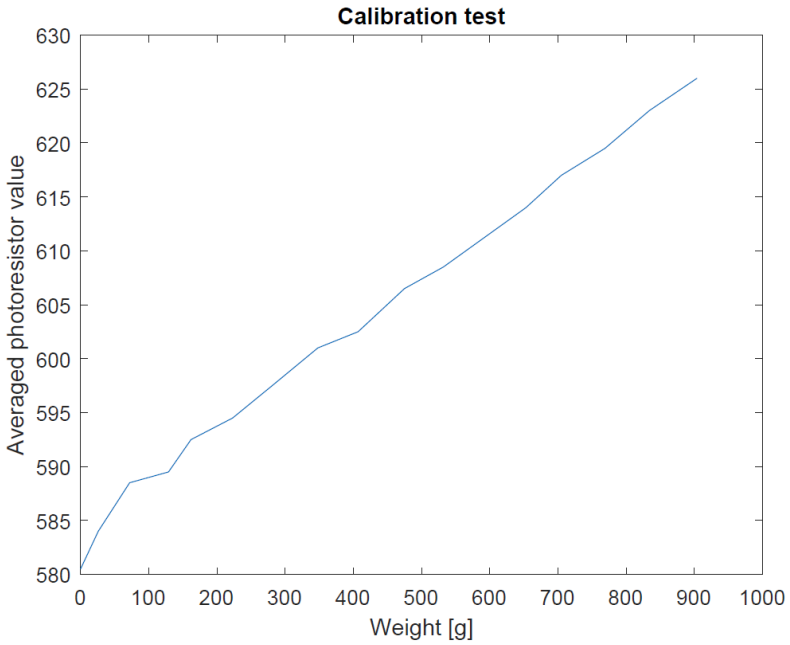

Fig. 7 Calibration test result: relation between weight on a single OPT-IN cell and the corresponding photoresistor voltage, shown here by its 10-bit digital conversion.

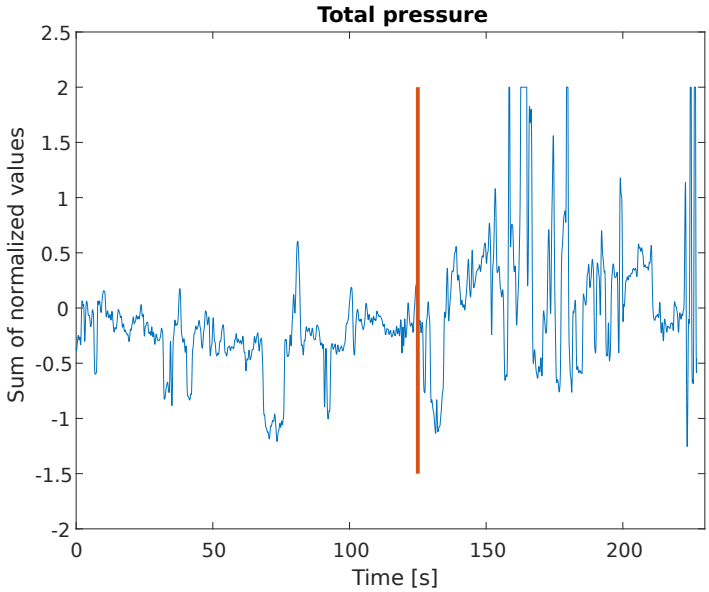

Fig. 8 Verification experiment: total pressure exerted on the OPT-IN sensorized inceptor grip during a 225 seconds mission divided into a cruise flight phase and a precision hovering phase

The setup is shown in Fig. 9. An experienced professional pilot has been involved in the flight test campaign. Tasks

Fig. 9 Test campaign setup including the motion platform, the sensorized inceptor grip and the monitors for glass cockpit visualization.

involve the tracking of a target both with cyclic and collective inceptors. The pilot executed the MTE by looking at the target shown on the screen, represented by a dot that moved on a plane following a pre-determined path. Another dot is controlled by the pilot and moves according to the motion of the cyclic stick (horizontal motion controlled by lateral input, vertical motion controlled by longitudinal input). A similar configuration is created for the collective inceptor, in which the path of the target is vertical. An example of the PFD screen is shown in Fig. 10:

The goal is to make the two dots related to the cyclic input and the two of the collective one overlap as much as possible throughout the entire duration of the MTE. The tests were designed to be increasingly more demanding, also including motion of the base with different intensities:

- a longitudinal mono-harmonic oscillation of fixed amplitude, repeated with increasing frequency;
- a lateral mono-harmonic oscillation of fixed amplitude, repeated with increasing frequency;
- a longitudinal sweep of fixed amplitude and increasing frequency;
- a lateral sweep of fixed amplitude and increasing frequency;
- a longitudinal and lateral mono-harmonic oscillation with different amplitude and frequency.
- The previous test is then repeated with the motion of the platform with the following disturbance:
  - vertical vibration, repeated at increasing frequencies;
  - vertical random disturbance.
- Cyclic and collective steady position maintenance with the following disturbance:
  - vertical random;
  - longitudinal random;
  - lateral random;

The detailed description of the test campaign is reported in Table 2.

To evaluate the workload of the different runs, the results obtained from the OPT-IN sensors system are used. Data are acquired at 1024 Hz.

Data are filtered with a fifth-order Butterworth low pass filter with a cut frequency of 20 Hz. The obtained signals are manipulated to extract:

- the total pressure exerted on the grip, given by the sum of the four sensors;
- the total longitudinal pressure exerted on the grip, given by the sensors on the front and on the back;
- the lateral pressure exerted on the grip, given by the sensors on the right and on the left;

Also, the mean of the absolute value of the three measurements above and their variance are computed. Finally, the Fourier transform is calculated as well to verify that the filtered and elaborated signals still contain the relevant components associated with the base excitation. As shown in Fig. 11, the OPT-IN sensors system is capable of collecting all the relevant frequencies, as well as the vibration of the platform, given that test 10 implied a 3.5 Hz base oscillation.

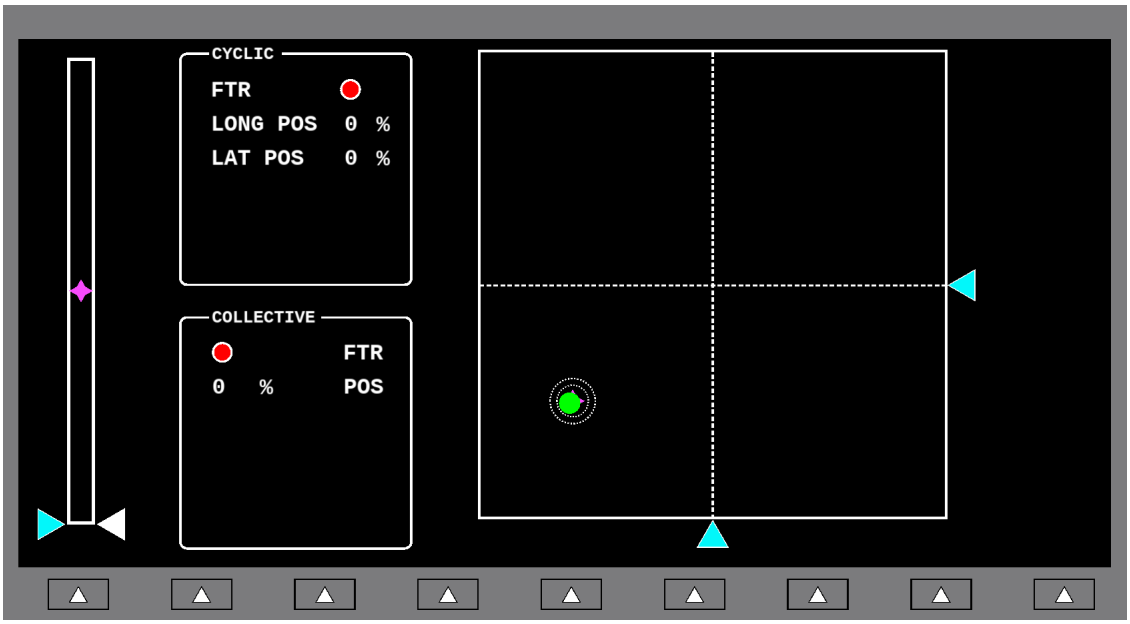

Fig. 10 **Tasks environment: the left column shows the target and the current position of the collective stick; the plane on the right shows the target and the current position of the cyclic stick. Overlapping percentage between target and current position are shown in the two boxes**

Table 2 **OPT-IN Test campaign recap**

	Task						**Motion base Disturbance**					
	Long		**Lat**		**Coll**		**Long**		**Lat**		**Vert**	
Tag	**Ampl**	**Freq**	**Ampl**	**Freq**	**Ampl**	**Freq**	**Ampl**	**Freq**	**Ampl**	**Freq**	**Ampl**	**Freq**
01	0,2	0,17										
02	0,2	0,5										
03			0,2	0,17								
04			0,2	0,5								
05			0,2	1								
06	0,2	0,17	0,2	0,1								
07	0,2	0,17	0,2	0,1	0,2	0,12						
08			0.2	0,1-2								
09	0,2	0,17	0,2	0,1	0,2	0,12					0,004	2,5
10	0,2	0,17	0,2	0,1	0,2	0,12					0,002	3,5
11	0,2	0,17	0,2	0,1	0,2	0,12					0,0012	4,5
12	0,2	0,17	0,2	0,1	0,2	0,12					0,1	rand
13	0,02	0,17	0,02	0,1	0,02	0,12					0,1	rand
14	0,02	0,17	0,02	0,1	0,02	0,12	0,1	rand				
15	0,02	0,17	0,02	0,1	0,02	0,12			0,1	rand		

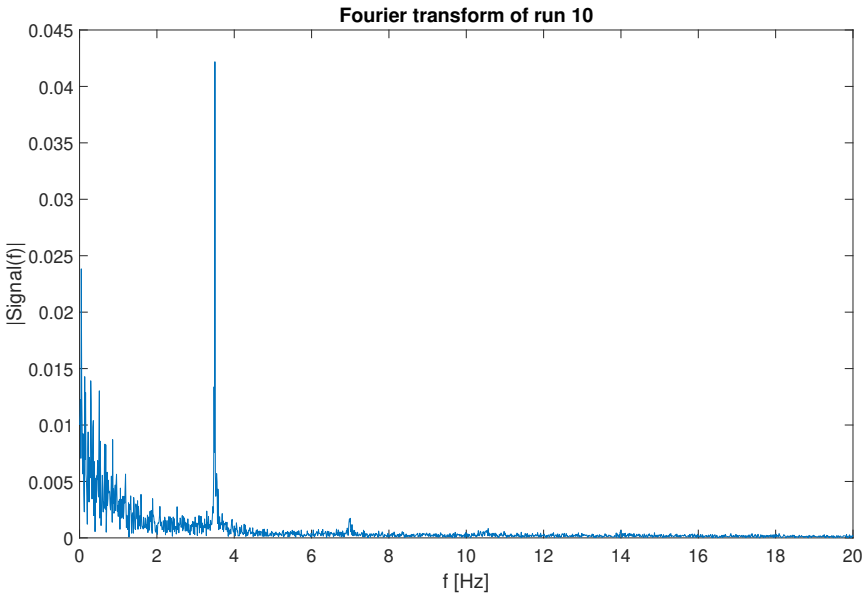

Fig. 11 Fourier transform of total pressure exerted on the OPT-IN sensorized inceptor grip during run 10. Peak at 3.5 Hz correspond to the motion base disturbance frequency of the specific test, which is correctly measured by the OPT-IN system

VI. Results

The collected data from the OPT-IN sensor system are used to obtain a measurement of the workload. In particular, after the filtering, the raw signals are given as shown in Fig. 12 taken as an example task for a mono-harmonic longitudinal motion.

The workload is quantified in relation to the mean value of total pressure exerted on the inceptor grip, and its variance. Comparison among signals shows that mean value and variance increase with the workload associated with the specific test.

As an example, if tests 3, 7 and 11 are considered, an increase workload is expected between tests 7 and 11, since they represent the same MTE done with and without a disturbance from the platform respectively. Also, test 3 is expected to have a lower workload due to the involvement of the longitudinal cyclic only. Predictions are confirmed by tests results as shown in 13a and 13b, where mean values and variances are represented for total pressure, longitudinal pressure and lateral pressure, referred to the three considered tests.

In 14a and 14b, the relevant values are given for all the tests, showing a general relation between the higher values of both variance and mean, and the expected workload of the MTEs.

VII. Conclusions and future developments

An assessment of current best practices in the online evaluation of pilot workload was performed analyzing data collected during a SHOL simulator test campaign performed at Leonardo Helicopters AWARE test facilities, involving deck landing operations of medium-sized helicopters on a Sirio class frigate. The pilot activity on the control inceptors was analized using a moving descriptive statistics approach. The statistical indicators gave the best results when applied to the control inceptors velocities, obtained by numerical differentiation of the original signal. Various indicators resulted in comparable levels, as measured by their Pearson correlation coefficient with the Bedford scale workload rating of the pilot. The best performances were obtained by the well-established aggression criterion and by the moving median of the absolute deviation from the moving average of the input signals.

Further development of the analysis presented in this paper will be focused on introducing time-frequency based methods, based on the Wavelet transform of the input signals, to capture the frequency content of the transient signal in bands that are associated with greater piloting effort.

An original approach to online pilot workload assessment is presented in the second part of the paper: an optical

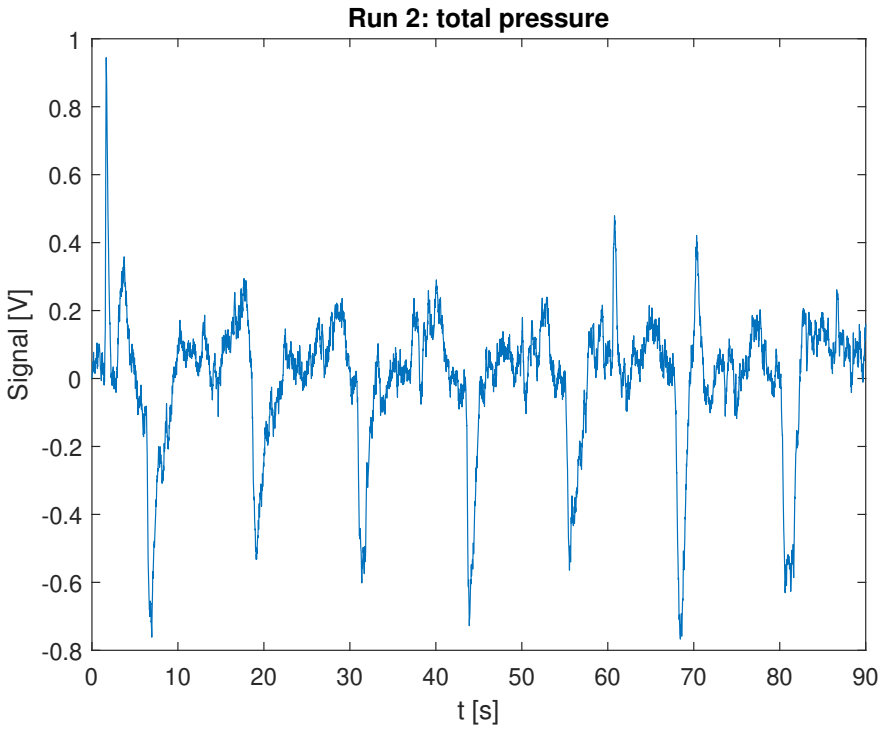

Fig. 12 Total pressure exerted on the inceptor grip during run 2. The periodicity of the target motion is visible in the result

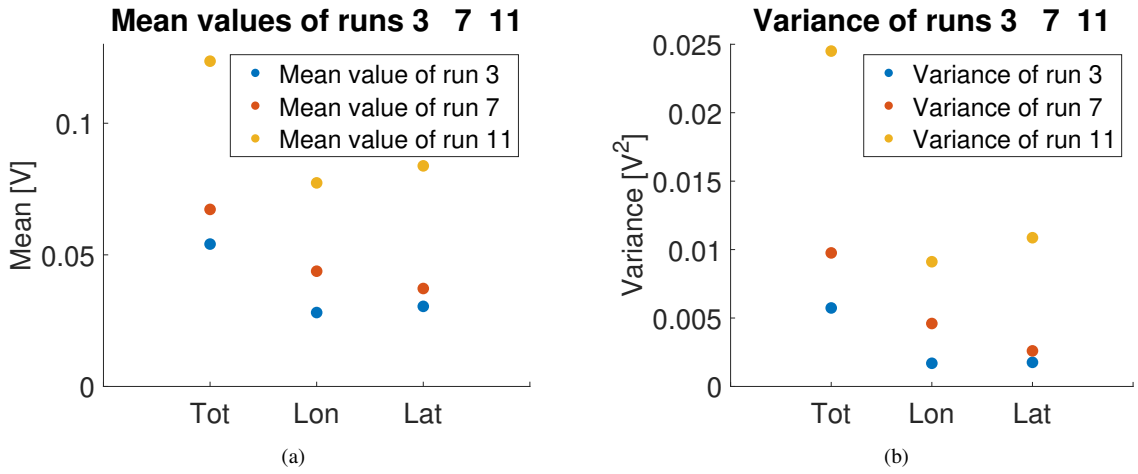

Fig. 13 Comparison among mean (13a) and variance (13b of the exerted pressure on the inceptor grip during runs 3, 7, 11 of Table 2: variance of total, longitudinal and lateral pressure signals are shown

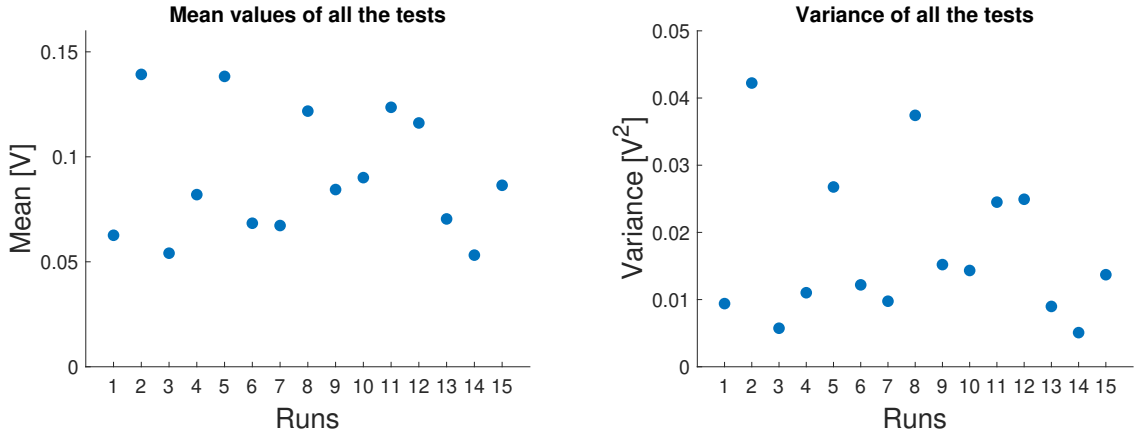

Fig. 14 Mean value (14a) and variance (14b) of the total pressure exerted on the OPT-IN sensorized inceptor grip for each of the 15 tests

hand-grip pressure sensing device, based on the Frustrated Total Internal Reflection of light principle, has been developed and integrated into the cyclic grip of the FRAME-Lab pilot-rotorcraft interaction testbed. A first test campaign, performed by a professional pilot and involving simple tracking tasks, has been performed. As the workload required by the pilot increased, also the mean total pressure exerted on the grip has been found to increase. Furthermore, the signal related to the pressure contains detailed information about the pilot hand activity. The early results show promising traits, thus further investigation on the possible applications of the OPT-IN sensors are envisioned in the future, starting with a more comprehensive test campaign involving multiple pilots and more complex tasks.

Acknowledgments

This work has been partially developed within the project RoCS (Rotorcraft Certification by Simulation) that received funding from the Clean Sky 2 Joint Undertaking (JU) Framework under the grant agreement N.831969. The JU receives support from the European Union's Horizon 2020 research and innovation programme and the Clean Sky 2 JU members other than the Union.

References

[1] Roscoe, A., and Ellis, G., "A subjective rating scale for assessing pilot workload in flight: A decade of practical use," TR 90019, Royal Aerospace Establishment, 1990.

[2] AA.VV., "Annual safety review 2020," Tech. Rep. TO-AA-20-001-EN-N, European Union Aviation Safety Agency (EASA), Cologne, DE, 2020. https://doi.org/10.2822/147804.

[3] Pavel, M. D., Jump, M., Dang-Vu, B., Masarati, P., Gennaretti, M., Ionita, A., Zaichik, L., Smaili, H., Quaranta, G., Yilmaz, D., Jones, M., Serafini, J., and Malecki, J., "Adverse rotorcraft pilot couplings — Past, present and future challenges," *Progress in Aerospace Sciences*, Vol. 62, 2013, pp. 1–51. doi:10.1016/j.paerosci.2013.04.003.

[4] Quaranta, G., Masarati, P., Lanz, M., Marforio, M., and Muscarello, V., "Biodynamic Adverse Rotorcraft-Pilot Coupling," *5th International Conference on Applied Human Factors and Ergonomics (AHFE 2014)*, AHFE, 2014, pp. 87–96.

[5] Venrooij, J., Abbink, D. A., Mulder, M., van Paassen, M. M., and Mulder, M., "Biodynamic feedthrough is task dependent," *2010 IEEE International Conference on Systems Man and Cybernetics (SMC)*, Istanbul, Turkey, 2010, pp. 2571–2578. doi:10.1109/ICSMC.2010.5641915.

[6] Jones, M., Jump, M., and Lu, L., "Development of the Phase-Aggression Criterion for Rotorcraft Pilot Couplings," *J. of Guidance, Control, and Dynamics*, Vol. 36, No. 1, 2013, pp. 35–47. doi:10.2514/1.58232.

[7] Zanoni, A., Zago, M., Paolini, R., Quaranta, G., Galli, M., and Masarati, P., "On Task Dependence of Helicopter Pilot Biodynamic Feedthrough and Neuromuscular Admittance: An Experimental and Numerical Study," *IEEE Transactions on Human-Machine Systems*, 2021, pp. 1–11. https://doi.org/10.1109/THMS.2020.3044971.

[8] Casner, S. M., and Gore, B. F., "Measuring and Evaluating Workload: A Primer," Tech. Rep. NASA/TM-2010-216395, NASA, Ames Research Center, Moffett Field, CA, USA, 2010.

[9] Quaranta, G., van't Hoff, S., Jones, M., Lu, L., and White, M., "Challenges and Opportunities offered by Flight Certification of Rotorcraft by Simulation," *Proceedings of the 47th European Rotorcraft Forum*, Royal Aeronautical Society, Virtual Event, 2021.

[10] Forrest, J. S., Hodge, S. J., Owen, I., and Padfield, G. D., "Towards fully simulated ship-helicopter operating limits: The importance of ship airwake fidelity," *AHS 64th Annual Forum*, Montréal, Canada, 2008.

[11] Garbo, P., Zanoni, A., Lavatelli, A., and Quaranta, G., "Sensore di pressione ottico," , May 24 2021. Patent Application P3736IT00.

[12] Bowditch, N., *American Practical Navigator: an epitome of navigation*, Vol. 2, Defense Mapping Agency Hydrographic Center, 1975.

[13] Forrest, J., Owen, I., Padfield, G., and Hodge, S., "Ship-helicopter operating limits prediction using piloted flight simulation and time-accurate airwakes," *Journal of Aircraft*, Vol. 49, No. 4, 2012, pp. 1020–1031. https://doi.org/10.2514/1.C031525.

[14] Zanoni, A., Zago, M., Paolini, R., Quaranta, G., Masarati, P., Galli, M., Maisano, G., Frigerio, L., and Murawa, M., "Biodynamic Testing for the Prediction of Rotorcraft-Pilot Couplings," *75th Annual Forum of the Vertical Flight Society*, Philadelphia, PA, USA, 2019.

[15] Zanoni, A., Zago, M., Paolini, R., Quaranta, G., Masarati, P., Galli, M., Maisano, G., Frigerio, L., and Murawa, M., "Flight Simulator Testing to Enhance Comprehension and Modeling of Rotorcraft Pilot Couplings," *45th European Rotorcraft Forum*, Warsaw, Poland, 2019.

[16] Garbo, P., Zanoni, A., and Quaranta, G., "An optical pressure measurement system for control inceptors to evaluate pilots' workload," *4th International Conference on Human Systems Engineering and Design: Future Trends and Applications (IHSED 2021)*, Virtual Event, 2021.